Interface parameters of composite sprayed concrete linings in soft ground with spray-applied waterproofing

Authors:

- Jiang Su[1]
- Alan Bloodworth[2]

Affiliations:

(1) Tunnels, AECOM, Croydon, UK

(2) School of Engineering, University of Warwick, UK

Abstract:

The presence of a spray-applied waterproofing membrane between the primary and secondary lining layers is important to the behaviour of a composite sprayed concrete lined (SCL) tunnel in soft ground. In order to confirm the feasibility of the composite shell lining concept, the structural adequacy of the concrete-membrane interfaces under the effects experienced in a typical tunnel needs to be investigated.

This paper presents a series of laboratory tests on samples cut from composite sprayed concrete panels, to which uniaxial compression, direct tension and direct shear loadings are applied over both short- and long-term timeframes under conditions of ambient atmospheric humidity. Test results show that the interfaces are capable of resisting significant compression, tension and shear in both short- and long-term. Failures under these actions should not occur in a typical shallow SCL tunnel, and a degree of composite action between primary and secondary layers should be expected. Influence of substrate roughness and membrane thickness on the measured interface properties has been quantified. Overall, this investigation confirms the existence of composite action for composite sprayed concrete linings in soft ground, and provides parameters based on test results for further research and design.

1 Introduction

Sprayed concrete lining (SCL) is an established tunnelling method used in many countries for the creation of underground space (Kovári, 2003a, 2003b). Traditionally, SCL tunnels consist of a layer of sprayed primary lining (considered as temporary works, not part of the permanent structure), a layer of sheet waterproofing membrane and a layer of cast secondary lining, regarded as the permanent load-bearing structure (Thomas, 2009; Institution of Civil Engineers, 1996). The tunnelling industry has long expressed concern about over-excavation and material waste due to the primary lining being treated as sacrificial in the long term (Duarte et al., 2012), and there have been rapid developments in the UK over the last twenty years to tackle this issue.

One of these was the inclusion of the primary lining in the permanent structure, sometimes with addition of a second sprayed layer, but known as a *single shell lining* (Grose and Eddie, 1996; Watson et al., 1999). Although this solution was cost-effective to construct, long-term problems associated with leaks and maintenance has pushed the industry back to including a waterproofing membrane. This option, consisting of a permanent sprayed concrete primary lining, sheet or spray-applied waterproofing membrane and sprayed or cast secondary lining, but with no adhesive and shear bond assumed at the concrete-membrane interface, is called a *double shell lining*, and has been adopted for several projects such as the A3 Hindhead Tunnel (Peynolds, 2008) and Crossrail (Su and Thomas, 2014) in the UK.

Whilst efficiency gains may be achieved with double shell linings compared to sacrificial primary linings for some cases, there is a desire for further improved lining thickness efficiency by utilising the adhesive and shear bonds at the concrete-membrane interface. This option, consisting of a permanent sprayed concrete primary lining, spray-applied waterproofing membrane and sprayed or cast secondary lining, with assumption of a degree of adhesive and shear bond ("composite action") across the interfaces, is called a *composite shell lining* (Pickett and Thomas, 2011; ITAtech, 2013).

For the moment, there is still uncertainty about the properties of the concrete-membrane interface. Therefore, there is scope for further investigation into the properties of the concrete-membrane interfaces to substantiate the function of composite shell linings. A summary of the key aspects of

each lining configuration with particular regard to how short and long-term ground loading and water pressure is shared between the lining layers is given in Table 1.

Table 1

Lining and interface loading scenarios for different SCL tunnel configurations

Lining configuration	Composite action between layers	Load sharing assumptions		
		Short-term loading	Long-term consolidation loading	Long-term water pressure
Single Shell Lining	N/A	All on the single layer	All on the single layer	All on the single layer
Double Shell Lining	None	All on the primary lining	Shared between two linings	All on the secondary lining
Composite Shell Lining	Partial or full composite	All on the primary lining	Shared between two linings	Shared between two linings

Until now, only a limited number of test results on interface properties with spray-applied waterproofing membrane have been reported, most of which refer to an ethyl-vinyl-acetate (EVA) based membrane (MasterSeal 345) under normal atmospheric moisture conditions (Verani and Aldrian 2010). Nakashima et al. (2015) presented flexural test results on two composite shell lining beams with and without axial force under normal ambient humidity condition. No information has been given with regards to the mechanical properties of the spray-applied waterproofing membrane interface. Field measurements by Holter and Geving (2015) on an SCL tunnel in rock with spray-applied waterproofing found the moisture content of the membrane to vary between 30% and 40%, determined by the moisture properties of the concrete and the membrane, as well as the interfaces between the two materials. Further research by Holter (2016) suggested that high moisture content in the membrane may affect its mechanical properties, e.g. reduce its tensile strength. In the research reported in this

paper, we have also assumed the membrane to be essentially dry (i.e. subject only to normal atmospheric humidity) as the best estimate of conditions in typical soft ground tunnelling for two main reasons. Firstly, the very low permeability of modern sprayed concrete, and extensive grouting normally carried out to seal primary lining cracks prior to application of the membrane, would substantially slow the rate of supply of moisture to the membrane. Secondly, the hotter temperature inside the tunnel would draw moisture from membrane into the tunnel where it would evaporate into the air. In the event of a structural crack occurring in the primary lining, groundwater could contact the membrane and increase its level of saturation. However, this would be a localised effect not significant to the tunnel as a whole provided the tensile bond between the membrane and the primary lining exceeds the water pressure and thus prevents the membrane debonding from the primary lining and allowing groundwater to contact a wider area of membrane.

Confirming the feasibility of the composite shell lining concept requires a thorough understanding of the fundamental properties of the concrete-membrane interfaces under conditions representative of those in the actual tunnel and derivation of appropriate parameters for input into numerical models for design. A testing programme has been carried out with these objectives, on samples cut from composite shell test panels, including quantifying the impact of substrate roughness and membrane thickness on interface properties. This paper reports the test methods and the results obtained and their significance, referring to another EVA-based waterproofing membrane (*TamSeal 800*). This product contains more than 75% by weight of EVA co-polymer, and its functional properties are expected to be similar to other EVA-based membranes.

2 Loading conditions of the membrane interface in a composite SCL structure

Behaviour of the primary and secondary linings, in particular the distribution of bending moment and axial force, is affected not only by ground and water pressures but also the properties of the interface between the layers. As a result of the global actions on the tunnel, the interface itself may experience tension or compression, either of which may be in combination with shear, at different locations around the tunnel.

An initial investigation into the behaviour of an idealised composite SCL tunnel under external loadings was carried out using Finite Difference software FLAC. The model consists of two circular rings in solid elements representing the primary and secondary linings, with an interface with normal stiffness of 17 GPa/m and shear stiffness of 8.7 GPa/m (Verani and Aldrian 2010, Table 2 Specimen 0) assigned in between to represent the spray-applied membrane. Both solid and interface elements are assumed elastic. Unequal vertical and horizontal loads at a ratio of 2:1 (1000 kPa : 500 kPa) were applied, as shown in Figure 1(a), and Figure 1(b) shows the general form of the lining deformation that resulted.

Ovalisation of the tunnel as shown in Figure 1(b) implies development of compressive stress in the interface between the primary and secondary linings at the crown and invert, and tensile stress at axis level. Relative shear between the lining layers will be greatest at the intermediate positions, although the maximum interface shear displacement observed was less than 1 mm. Different loading conditions (*e.g.* greater value of K_0) may change the lining deformation pattern and distribution and magnitude of interface stresses, but the interface should still experience these three stress conditions at different locations.

3 Laboratory tests and testing parameters

3.1 Laboratory tests and interface properties

In response to this fact, three types of laboratory test were conducted on samples cut from composite sprayed panels: (a) uniaxial compression, (b) direct tension, and (c) direct shear. The interface properties sought under each of these actions were peak and post-peak strengths, and short- and long-term stiffnesses. Adequate interface peak strength and ductile post-peak behaviour give confidence that the composite shell lining would be robust and maintain its integrity under ground loading, with ductility important in resisting sudden loading changes, such as those caused by excavation in close proximity or construction of cross-passages. There is an additional requirement on the tensile strength that it should exceed the likely possible groundwater pressure, so that in the event of a localised crack in the primary lining allowing water to reach the membrane, no debonding occurs which could allow the groundwater pressure to load a wider area of membrane.

Interface stiffness values under all three actions are sought as input to numerical models to accomplish tunnel analysis and design. The shear stiffness is key in determining the degree of composite action between the primary and secondary linings, whilst the normal (compression and tension) stiffnesses influence the amount of load that can be transferred between the primary and secondary linings at the locations where the interface is under normal stress as described in the previous section.

Each test type was carried out under both short- and long-term loading. In the long term, the interface may relax gradually, leading to a reduced apparent stiffness and degree of composite action for a composite SCL tunnel. A long-term relaxation ratio is defined (for each loading condition) as the long-term interface stiffness as a percentage of the short-term.

3.2 Testing parameters

The ranges of parameters for the tests under the three types of action given above are now described.

In compression, samples were loaded until failure and the peak stress recorded. From the stress-displacement relationship, the first loading stiffness was obtained as a measure of the stiffness at low load for input into a numerical model. In addition, samples were taken through unload-reload cycles between approximately 10% and 50% of peak stress (once this was known) to ascertain the likely degree of hysteresis and degradation of stiffness with stress at levels indicative of the maximum likely to which the lining would be loaded in practice.

In the long-term compression test, confirmation was sought that the lining system could resist the maximum theoretical full overburden pressure, and so sufficiently large stresses of 3 MPa, 6 MPa and 15 MPa (representing overburdens up to 750 m) were applied and each held for a period of time.

In the tensile tests, samples were loaded up to 0.6 MPa (representing a ground water head of 60 m which exceeds the likely maximum in most soft ground tunnelling projects) to obtain the first loading stiffness. The load was then cycled between 0.1 MPa and 0.6 MPa to explore any degradation of stiffness with cycles, before loading to failure to obtain peak stress. In the long term test, a stress of 0.5 MPa was applied to represent a depth below water table of 50 m, and held.

Direct shear tests were carried out under normal stresses of 250 kPa, 500 kPa and 750 kPa, representing full overburdens on tunnels in the range 15-40 m below ground. Pickett & Thomas (2011) indicate that a shear strength of 2 MPa is sufficient in “no-slip” full composite action scenarios. A

lower strength may be adequate in cases of partial composite action, and the actual strength requirement could be confirmed in a numerical model once the interface stiffness parameters are understood, which is an aim of this paper. Samples were sheared to around 0.7 MPa shear stress to obtain first loading shear stiffness, the stress reduced to 0.2 MPa and then samples taken through progressively increasing stress cycles until peak stress is reached, to again explore stiffness degradation and the impact of machine compliance. In the long term test, a shear stress of 1 MPa was applied and held.

4 Procurement of test samples

4.1 Sample mix and spray

A contractor was commissioned to produce fifteen panel boxes, 800 mm×800 mm or 800 mm×1000 mm in size and 200 mm deep. Sprayed concrete mix specification and design are given in Tables 2 and 3 respectively. An EVA-based waterproofing membrane (*TamSeal 800*) was used. The spray was carried out at the contractor's plant facility and the direction of all spray was perpendicular to the test box (Figure 2) (BS-EN 14487-1, 2005).

Table 2

Mix specification for primary and secondary lining sprayed concrete

Mix	Description	Agg Size (mm)	Cement Type	Targeted Slump	Targeted 90-day Strength
20080778	P450 HP-PLA sprayed concrete mix	8	CEM1	S3	40MPa

Table 3

Mix design for primary and secondary lining sprayed concrete

Materials		DRY Batch Weights kg/m^3
Type	Source	20080778

CEM1	Cemex- Rugby	450
0/4 MP Sand	Cemex - Northfleet	1300
4/10 Gravel	Cemex - Northfleet	550
WRA (N)	Cemex – CP105 (ml)	2250
Target W/C	Target Water/Cement Ratio	0.45
Steel fibre	Dramix	40
Accelerator	Tamshot 800	6% (weight of cement)
Superplasticiser	TamCem 60	0.9% (weight of cement)

4.2 Sample panel specification

The primary layer was first sprayed to approximately half of the boxes' depth and then finished in one of three ways typically used in SCL tunnel projects (Figure 3): (i) *as-sprayed* with relatively rough surface and fibers protruding; (ii) *float finish* (where the standard material is worked immediately after spraying to give a smooth flat finish) and (iii) *regulated finish*. The latter was achieved by returning a few days after primary lining spray and dry-spraying a finer, fiber-free material (in this case *TamCrete Topshot*), without further working or smoothing. Regulated finish has been recommended by both a designer and material supplier where spray-applied waterproofing membrane is to be applied, as it enables application of a regular thickness of membrane without the need to work at height first to achieve a "plaster-smooth" finish to the primary lining (Crossrail, 2009; Dimmock et al., 2011). The primary layer was cured for 28 days.

The membrane material is supplied as dry powder that is mixed with water using a dry-rotor machine. The powder/water ratio is set to ensure full polymerisation, typically at 1.75:1. The membrane was applied in two layers, the first coloured orange and the second applied a short while later coloured white/grey, as recommended by Normet (2011) to enable greater quality control of the application. Two target membrane thicknesses were aimed for in this project: (i) *thin* membrane (<=4 mm), representing the ideal best practice; and (ii) *thick* membrane (>4 mm), representing a non-ideal scenario of over-sprayed membrane. Achievable membrane thickness can be expected to relate to substrate roughness: where the substrate is uneven, it will be impossible to apply the consistently thin

layer achievable on a smoother surface. The membrane achieves initial set after only a couple of hours, but was left for 48 hours to ensure complete curing before the secondary lining was applied. A secondary sprayed concrete layer (the same fibre-reinforced mix as the primary lining) was then applied directly to the membrane surface that had been dampened in accordance with manufacturer's recommendations. The secondary lining was also cured for 28 days.

After each spray, the boxes were covered with plastic sheeting to prevent exposure to sunshine or cold air, simulating a realistic environment for sprayed concrete curing in the underground. The spray was carried out during the summer (June –August 2011) in the UK, with daily temperatures ranging from 15-25 °C.

4.3 Test sample preparation

Once spraying and curing were completed, the sprayed concrete panels were cored and cut to obtain cylinder, cube and beam samples. Only the tests on cylinder and cube samples are presented in this paper. Beam samples were tested later once the basic compression, tension and shear behaviour of the interfaces was known, to calibrate a numerical simulation approach for a composite shell lining, which is the subject of a future paper.

Cylinders with a diameter of 100 mm and a nominal height of 200 mm were desired for compression and tension testing, as recommended by BS-EN 12390-1 (BSI 2000). However, due to the necessity of removing the uneven top surface resulting from the secondary lining spraying, actual heights of the cylinders varied between 180-190mm, but this height difference was thought to only make a small difference of ~2% to test results compared to standard dimension samples (Neville 2011, Table 12.1). Target dimensions for cube samples were 200×200×200 mm. Typical 'thin' membrane cylinder and cube samples are shown in Figure 4.

Test samples were coded with two numbers, the first being the Sample Type, which indicates the combination of interface finish and measured membrane thickness that comprise the interface characteristics (Table 4), and the second the sample number within its Type. For example, Sample 2-6 is the 6th of the Type 2 samples. The three different types of interface finish are illustrated in Figure 3.

Table 4

Sample designation: Interface characteristics

Sample Type	Interface finish (substrate roughness)	Range of measured membrane thickness (mm)
Type 1	Smooth	1-4
Type 2	Regulated	1-4
Type 3	As sprayed	1-4
Type 4	Smooth	4-12
Type 5	Regulated	4-12
Type 6	As sprayed	4-12

5 Test programme and methodologies

5.1 Testing programme

Nine test configurations covered short- and long-term uniaxial compression, direct tension and direct shear, as listed for each Sample Type in Table 5.

Table 5

Numbers of samples for each test configuration

Test Configuration	Type 1	Type 2	Type 3	Type 4	Type 5	Type 6	Total number
Short-term compression	3	3	3	2	3	3	17
Long-term compression	1						1
Short-term direct tension	3	3	2	3	3	2	16
Long-term direct tension		1					1
Short-term direct shear (500 kPa)[a]	3	3	3	3	3	3	18
Short-term direct shear (250 kPa) [a]	3	3		3	3		12
Short-term direct shear (750 kPa) [a]		3					3

Long-term direct shear (500 kPa) [a]	1	1
Long-term direct shear (250 kPa) [a]	1	1

[a] Applied normal pressure in direct shear tests

5.2 Uniaxial compression test

The setup is shown in Figure 5. Load was applied using a servo-hydraulic machine with 650 kN capacity. Three potentiometers were arranged symmetrically around the sample, positioned between two aluminium rings attached to the sample to measure local change in length across the interface, over a gauge length of approximately 160 mm. Machine load and stroke position were logged once per second, along with potentiometer output. All tests were performed in stroke control mode.

For short-term tests, firstly one sample was taken and loaded in compression up to 10 MPa average stress to obtain the first loading stiffness. An unload-reload cycle down to 2 MPa and back to 10 MPa was then applied to obtain the cyclic loading compressive stiffness and check for hysteresis. This was repeated twice more to obtain an average value of cycle loading stiffness. After that, load was increased until the samples started to fail and stress started to drop. Stroke rate was maintained at 0.01mm/s throughout.

This first test on a sample of each type indicated its general behaviour and compressive strength. For the remaining samples of each type, the test procedure was basically the same but with upper and lower bounds of the load-unload cycles fixed at 50% and 10% of the compressive strength found from the first sample.

Long-term uniaxial compression tests were carried out for just one Type 1 sample (1-1), as relaxation is believed not to be influenced by substrate roughness or membrane thickness, but only by the molecular structure and physical properties of the membrane polymer (Ashby and Jones, 2005). The sample was loaded to progressively increasing target stresses of 3.0, 6.0 and 15 MPa, and once the target stress was reached, the steel loading plates were held stationary, allowing stress relaxation to happen over a period of one week. Laboratory temperature was continuously recording during the test.

The compression tests and their objectives are summarised in Table 6.

Table 6

Uniaxial compression test stages and objectives

Test stage	Description	Reason
1	Cyclic loading sample to 10 MPa and unloading to 2 MPa three times; Increase load until sample starts to fail and stress drops	Obtain first- and cyclic-loading interface compressive stiffness and check for hysteresis and stiffness degradation; Obtain interface compressive strength
2	Cyclic loading second and third samples three times between 50% and 10% of compressive strength from first sample	Obtain further first- and cyclic-loading interface stiffness and interface compressive strength values
3	Long-term relaxation test under 3.0, 6.0 and 15 MPa respectively held for one week.	Obtain long-term compressive relaxation ratio as a function of compressive stress

5.3 Direct tension test

The setup is shown in Figure 6. Direct tension was applied by means of steel plates 20 mm thick glued to the ends of the samples with epoxy adhesive, to which steel rods were welded perpendicular and held in the machine grips. Arrangement of potentiometers and data recording were the same as for the compression tests.

The short-term testing procedure was the same for all samples. Samples were firstly loaded up to 0.6 MPa, a stress level safely exceeding the likely maximum water pressure acting on a shallow tunnel, to obtain the first loading tensile stiffness. Stress was then reduced below 0.1 MPa and increased back to 0.6 MPa to complete an unload-reload cycle; this was repeated three times to obtain the average secant cyclic tensile stiffness. Stress was then increased until the samples started to fail and the stress began to drop. Stroke rate was maintained at 0.01 mm/s throughout.

A single long-term test was carried out, on a Type 2 sample, as substrate roughness and membrane thickness were discovered in the short-term tests to have little impact on tensile modulus, as discussed later. The sample was loaded up to 0.5 MPa and loading plates held fixed, allowing stress relaxation over a period of two weeks.

The tension tests and their objectives are summarised in Table 7.

Table 7

Uniaxial tension test stages and objectives

Test stage	Description	Objective
1	Cyclic loading three samples to 0.6 MPa and unload to 0.1 MPa three times; Increases load until the sample starts to fail and stress drops	Obtain first- and cyclic-loading interface tensile stiffness and check for hysteresis and stiffness degradation; Obtain interface tension strength
2	Long-term relaxation test under 0.5 MPa held for two weeks	Obtain long-term tensile relaxation ratio under likely maximum tensile stress due to groundwater pressure

5.4 Direct shear test

The direct shear tests were carried out in a large geotechnical shear testing machine (Wykeham Farrance, equipped with a Sercomp 7 Special hydraulic controller system). The shear machine has two loading systems, one for normal stress and one for shear stress, and comprises an upper box fixed stationary to the machine and a lower box pushed by two hydraulic rams to generate shear in samples (Figure 7). As the dimensions of the shear box, 300×300×200 mm, were larger than those of the cube samples, timber wedges were used to restrict the movement of the samples within the shear boxes. The Young's modulus of timber is around 10 GPa, leading to a stiffness for a 150 mm combined length timber wedge of 6.66 GPa/m, which is much higher than the first loading stiffness of the membrane interface (between 0.5-1.0 GPa/m). The impact of timber wedge compliance on the cyclic loading stiffness is therefore expected to be minimal after the first loading cycle. Once the test sample was positioned in the shear box and fixed by the timber wedges, the top cap was placed and followed by the crossbeam, through which normal stress was applied to simulate the tunnel overburden of 250 kPa, 500 kPa or 750 kPa.

A total of six LVDTs were calibrated and used to record data. One LVDT is located within a loading ring positioned to the rear of the machine to record shear load and another at the back of the lower shear box to measure its horizontal displacement. The remaining LVDTs were positioned at the four

corners of the top cap to measure vertical dilation and rotation of the sample. Normal force applied by the cross beam was also recorded continuously.

The short-term shear tests followed a similar pattern to the direct tension tests, in which the blocks were initially sheared to around 0.7 MPa to obtain first loading shear stiffness and then the stress reduced to 0.2 MPa for a complete cycle of load. Second and the third cycles of loading were then performed at progressively higher stress levels, each 0.3-0.4 MPa higher than the previous to obtain the average secant cyclic shear stiffness, before the sample was then sheared to failure, judged to be when the shear force started to drop. Shear stroke rate was 0.2 mm/min throughout.

For the long-term tests, two Type 2 samples, one under 500 kPa normal stress and the other under 250 kPa, were sheared to 1 MPa and then the shear displacement kept constant, allowing stress relaxation to occur over a period of two weeks. Laboratory temperature was recorded continuously by a probe adjacent to the shear box.

The direct shear tests and their objectives are summarised in Table 8.

Table 8

Direct shear test stages and objectives

Test stage	Description	Objective
1	Apply 500 kPa normal stress, then cyclic loading in shear all samples first to 0.7 MPa then unload to 0.2 MPa, then at progressively higher stress levels until sample starts to fail and stress drops	Obtain first- and cyclic-loading interface shear stiffness under 500 kPa normal stress and check for hysteresis, stiffness degradation and machine compliance; Obtain interface shear strength under 500 kPa normal stress
2, 3	Repeat stage 1 for applied normal stresses 250 MPa and 750 MPa	Obtain the first- and cyclic-loading interface shear stiffness and interface shear strength under 250 kPa and 750 kPa normal stress; Evaluate impact of normal stress on interface shear stiffness and strength
4	Long-term relaxation tests on two samples under 500 kPa and 250 kPa normal stress respectively	Obtain the long-term shear relaxation ratios under two normal stresses. Evaluate impact of normal stress on long-term interface shear relaxation ratio.

5.5 Post-processing and presentation of results

Three pure sprayed concrete cylinders of similar dimensions to the composite shell samples were tested in compression to obtain a short-term concrete Young's modulus of 20 GPa. This was used to correct for deformation of the concrete in the composite compression and tension specimens, so that the deformations reported are for the interface only.

In a trial long-term compressive test on a pure sprayed concrete cylinder sample, it was observed that the load fluctuated over time during the test in a manner that correlated with the recorded temperature adjacent to the machine. The load reduced by 1.5 MPa for each 1 °C temperature reduction. This relationship was used to adjust the raw long-term compression and tension relaxation test data in following sections.

The direct shear tests measured the shear displacements externally, which is affected by compliance of the testing machine and rotation of the shear samples during the test, which was corrected using the vertical LVDT's as mentioned above. This paper reports only the adjusted values after correction for these effects.

Test results are presented in terms of stress (direct or shear, applied load divided by gross loaded area) against deformation across the interface in millimetres. Derived interface parameters are the interface normal stiffness K_n and shear stiffness K_s obtained as the change in direct or shear stress respectively divided by the corresponding deformation, with units of GPa/m. The influence of substrate roughness and membrane thickness on K_n, K_s and failure stress is explored.

6 Results and discussion

6.1 Short-term uniaxial compression

Typical interface stress-deformation graphs for selected samples with thin (Types 1 to 3) and thick (Types 4 to 6) membranes are shown in Figures 8 and 9 respectively. All samples failed in a brittle manner after reaching peak stress. Peak stresses for Type 1 and 2 samples were distinctively higher than for other types. There was no obvious increase in cyclic stiffness with increase in stress level. Numerical data for all samples is given in the Appendix in Table A1, and statistical analysis in Table 9 below, which shows that mean peak stresses for Type 1 and Type 2 samples were very close, around 36-38 MPa, whilst the other sample types were grouped around 16-21 MPa. Thus, as-sprayed rough

interface reduces compressive peak stress by approximately 50% for samples with thin membrane (Type 3). A thick membrane also reduces the compressive peak stress by approximately 50%, and influence of substrate roughness is less (Types 4 to 6).

First loading stiffness increases with reduced membrane thickness and reduced substrate roughness, over the range 2 to 16 GPa/m approximately. Cyclic loading stiffness increases with reduced membrane thickness, over the range 20 to 80 GPa/m, but is little affected by substrate roughness. Thus influences of interface characteristics on stiffness are similar to on compressive peak stress.

Table 9

Statistical analysis of uniaxial compression test results

Sample Type	Peak stress		First loading stiffness		Cyclic loading stiffness	
	Mean (MPa)	Standard deviation (MPa)	Mean (GPa/m)	Standard deviation (GPa/m)	Mean (GPa/m)	Standard deviation (GPa/m)
Type 1	37.7	0.6	12.2	1.2	68.2	8.8
Type 2	36.3	3.8	19.1*	7.6*	65.4	6.9
Type 3	19.3	5.0	7.4	1.7	58.9	25.8
Type 4	20.5	4.9	2.9	0.5	32.4	1.4
Type 5	16.0	3.6	2.4	0.4	28.5	6.5
Type 6	17.7	6.0	4.7	2.1	61.5	20.9

* Mean and standard deviation of first loading stiffness become 14.7 GPa/m and 0.8 GPa/m respectively if Sample 2-1 is excluded

All compressive samples failed in transverse tension, with vertical cracks formed either side of the membrane, as shown in Figure 10. For samples with thick membrane, a significant quantity of membrane was squeezed out, pulling some of the surface concrete away with it (Figure 10(b)). This is likely to have induced horizontal tensile strain at the interface and be the reason why Types 4, 5 and 6 samples failed at lower stress levels that were less dependent on stress level than thin membrane samples.

6.2 Short-term direct tension

Typical interface stress-deformation relationships for selected samples with thin and thick membranes are shown in Figures 11 and 12 respectively. Numerical data is given in Table A2 and statistical analysis presented in Table 10. Peak tensile stress for all samples is above 0.75 MPa, well above the maximum pore water pressure a shallow SCL tunnel is likely to experience. Mean peak tensile stress for Type 2 samples is higher than for Types 1 and 3, and the standard deviation smaller, suggesting

Type 2 regulated interface produces more consistent and higher quality interfaces. Table 10 also shows that thick membrane and as-sprayed interface do not change interface peak tensile stress significantly. Thin membrane samples, with the exception of 1-6, showed a ductile stress plateau post-peak stress, able to maintain a stress of 0.4 MPa at 1.0 mm extension. Sample 1-6 failed in a brittle manner, the reason for which is unclear. However, it still achieved a tensile strength of 0.8 MPa. Thick membrane interfaces (Types 4 to 6) showed a more declining stress path (although still reasonable ductility), with seven out of eight samples able to sustain 0.4 MPa at a 1.5 mm extension. This ductile behaviour gives confidence to designers that the tunnel is able to response to sudden changes in loading (*e.g.* adjacent construction) during construction or the structure's life.

Table 10

Statistical analysis of direct tension test results

Sample Type	Peak stress		First loading stiffness		Cyclic loading stiffness	
	Mean (MPa)	Standard deviation (MPa)	Mean (MPa)	Standard deviation (MPa)	Mean (MPa)	Standard deviation (MPa)
Type 1	0.83	0.09	15.2	4.9	32.3	18.0
Type 2	1.06	0.08	130.0	81.5	68.0	28.4
Type 3	0.96	0.17	220.6	252.5	73.5	43.1
Type 4	0.90	0.14	13.5	5.5	25.7	9.8
Type 5	0.89	0.10	6.3	2.5	11.4	3.1
Type 6	0.99	0.07	34.5	0.3	53.1	0.7

Table A2 shows that with the exception of three outliers (samples 2-6, 2-7 and 3-5), first loading stiffness for all samples was below 60 GPa/m, mostly between 10 – 40 GPa/m and reducing with increased membrane thickness. The very high first loading stiffness for the three outliers was probably caused by imperfect vertical alignment of test samples and the very thin membrane thickness (between 1 – 3 mm). Table A2 also shows that except for two of the same outliers (2-6 and 3-5), cyclic loading stiffness was below 60 GPa/m, very similar to first loading stiffness and again reducing with increased membrane thickness.

For Type 2 and Type 5 samples with regulated interface finish, failure occurred by debonding of the membrane at the interface with the secondary layer, suggesting higher bond strength exists between membrane and regulating layer (Figure13(a)). Other sample types showed equal probability of membrane debonding from primary or secondary linings (Figure 13(b)). Rupture was not observed within the membrane itself.

6.3 Short-term direct shear under 500 kPa normal pressure

Typical stress-deformation relationships for selected samples with thin and thick membranes are shown in Figures 14 and 15 respectively. For thin membrane samples, peak shear stress occurred at a displacement of 8 –10 mm and all samples failed in a ductile mode. For samples with thick membrane, peak shear stress occurred at 10 – 15 mm displacement and samples also failed in a ductile way. This high degree of shearing ductility for all samples is sufficient to accommodate potential deformation experienced by a shallow SCL tunnel.

Numerical test results and statistical analysis are presented in Tables A3 and 11 respectively. With only one exception, all samples withstood a 2 MPa shear stress which is an upper estimate on the stress likely in an SCL tunnel suggested by Pickett & Thomas (2011). Amongst thin membrane samples, peak stress for Type 3 is greater than for Type 2, in turn greater than for Type 1. Thick membrane samples generally follow the same trend, albeit with lower peak shear stress, suggesting that the greater the substrate roughness and the thinner the membrane, the higher the peak stress. For thin membrane samples, mean first loading stiffnesses for Types 1 and 2 were smaller than for Type 3. The same trend was observed for thick membrane samples but with greater first loading stiffness values. This trend was also observed for cyclic loading stiffness values for samples with thick membrane, but not for samples with thin membrane, possibly due to the small number of samples.

Table 11

Statistical analysis of direct shear test results (under 500 kPa normal pressure)

Sample Type	Peak shear stress		First loading stiffness		Cyclic loading stiffness	
	Mean (MPa)	Standard deviation (MPa)	Mean (GPa/m)	Standard deviation (GPa/m)	Mean (GPa/m)	Standard deviation (GPa/m)
Type 1	2.46	0.18	0.64	0.17	3.69	1.49
Type 2	2.76	0.39	0.65	0.12	4.61*	1.28*
Type 3	2.91	0.57	1.00	0.06	5.38	2.37
Type 4	2.14	0.09	0.73	0.25	2.20	0.50
Type 5	2.26	0.09	0.50	0.12	1.61	0.29
Type 6	2.25	0.36	0.59	0.02	1.98	0.85

* Based on two test results

Observed failure mechanisms fell into categories of either interface shear failure or membrane cohesive shear failure. For samples with smooth or regulated interface finishes, both the thin and thick

membrane usually slid along one interface (with no preference as to which one), as shown in Figure 16 (a) and (b). For samples with rough as-sprayed interface, the membrane usually failed in a mixed mode, sliding over relatively smooth parts of the interfaces and shearing within the membrane at the rougher parts, as shown in Figure 16 (c) and (d). This suggests that the dominating failure mode is that of the interface, with shearing within the membrane considered a consequence or by-product of the interface failure.

6.4 Type 2 samples in short-term direct shear under other normal pressures

Additional short-term direct shear tests were carried out for Type 2 samples under 250 kPa and 750 kPa normal pressures as described in Table 5. All samples failed in a ductile mode with similar response in shear to samples under 500 kPa.

Statistical analysis of direct shear results for Type 2 samples under all three normal pressures are presented in Table 12. It can be seen that peak shear stress increases with increasing normal pressure. From this trend, effective cohesion and friction angle may be calculated for the sprayed concrete-membrane interface, giving values of 2.2 MPa and 48^0 respectively.

Table 12 also shows that normal pressure has little impact on the first loading shear stiffness for Type 2 interfaces, with an average value of approximately 0.6 GPa/m. Cyclic loading stiffness for samples under 250 kPa normal pressure is greater than for those under 500 kPa and 750 kPa. This counterintuitive result may be due to sample rotation, most pronounced for samples under the lowest normal pressure of 250 kPa, not having been fully corrected for.

Considering the 250 kPa values as outliers, it is concluded from the other results that normal pressure has little impact on the cyclic loading stiffness, which has an average value of approximately 4.4 GPa/m.

Table 12

Statistical analysis of direct shear test results for Type 2 samples under all normal pressures

Normal pressure (kPa)	Peak shear stress		First loading stiffness		Cyclic loading stiffness	
	Mean (MPa)	Standard deviation (MPa)	Mean (GPa/m)	Standard deviation (GPa/m)	Mean (GPa/m)	Standard deviation (GPa/m)
250	2.45	0.21	0.56	0.09	11.17	4.18
500	2.76	0.39	0.65	0.12	4.61*	1.28*
750	3.00	0.32	0.56	0.07	4.38	0.90

* Based on two test results

6.5 Long-term tests

In the long-term compression tests, the load relaxed to around 70-80% of its initial value after one week. A logarithmic trend of load reduction with time was obtained, from which a stress relaxation ratio of approximately 0.5 is predicted at 120 years, the design life for most underground tunnels in London.

The long-term tension test was analysed in a similar manner to the compression tests, and the stress relaxation ratio calculated as 0.46 at 120 years.

Long-term direct shear tests were carried out on two Type 2 samples, under normal pressures of 250 and 500 kPa respectively and a shear stress of 1 MPa. It was seen that the shear stress for both samples relaxed from 1 MPa to approximately 0.8 MPa over five days, at which there was a sudden drop of stress to about 0.2 MPa. Shear stress then continued to relax after that, but at a much lower rate, presumably because the normal stress had dropped. The stress drop was found to be an artefact of the shear box test machine, which automatically cut its vertical stress after five days as a safety feature. By combining the relaxation curves before and after the stress drop, two completed long-term stress curves were obtained, one for each normal pressure. Extrapolation of the relaxation trend to 120 years gave a stress relaxation ratio of around 0.6, very close to the compression and tension long-term ratios of 0.5 and 0.46. Output from the long-term test under 500 kPa normal pressure with the logarithmic fit to the load-time relationship is shown in Figure 17.

7 Interface parameters

Ranges of interface stiffness parameters K_n and K_s and peak strengths for design of composite SCL tunnels where the membrane is at normal atmospheric humidity (believed to the most likely conditions in soft ground) are proposed in this section. Upper and lower limits of each range are calculated from the experimental data mean and standard deviation as ±95% percentiles assuming normal distributions (*i.e.* mean ±1.64 standard deviations). Compressive and tensile normal stiffness K_n is estimated using first loading stiffness, because local measurement was adopted for these two tests. In contrast, shear stiffness K_s is estimated using cyclic loading stiffness, because global measurement was adopted for those tests so first loading stiffness is more affected by initial machine compliance. Shear stiffness was

shown to be independent of normal pressure, hence only one value is quoted for each specimen type, and K_s is reported as a single value for both smoothed and regulated substrates because their test results are very close. For numerical analysis of a long-term loading situation, it is suggested that a relaxation ratio of 50% is applied to all stiffness values.

The ranges of K_s in Table 13 broadly coincide with the realistic range of 0.1 – 1.0 GPa/m suggested by Pickett and Thomas (2011) for which partial slip of the secondary lining relative to the primary would be expected, but is below the range for no slip (>10 GPa/m). Thus a composite SCL tunnel with these interface properties should behave as a partially composite structure, with lining flexural stiffness from two to four times (*i.e*. non-composite to fully composite lining respectively) the stiffness of an individual lining layer if both linings are of the same thickness. The degree of composite action in theory depends to a certain extent (as indicated in the Table) on the interface characteristics of substrate roughness and membrane thickness, but its actual sensitivity in a real tunnel situation to value of K_s chosen from the ranges given in the Table requires confirmation in a numerical model, which is the subject of further research to be reported in a future paper.

Table 13

Suggested ranges of interface stiffness parameters (short-term*) for composite shell lining design, assuming spray-applied waterproofing membrane (*TamSeal 800*)

Interface Type	Compression K_n GPa/m	Tension K_n GPa/m	Shear K_s GPa/m
Thin membrane, smoothed or regulated layer	10 – 16	7 – 23	0.3 – 6.7
Thin membrane, as-sprayed layer	4 – 10	7 – 23	0.9 – 9.3
Thick membrane, smoothed or regulated layer	1 – 4	2 – 22	0.3 – 3.0
Thick membrane, as-sprayed layer	1 – 8	2 – 22	0.5 – 3.3

* A suggested relaxation ratio of 50% should be applied to all stiffness values for long term loading

Suggested minimum (lower 95% percentile) interface peak strengths are given in Table 14. Tension and shear values are sufficient to ensure bond is maintained between the concrete layers and waterproofing under all conditions likely to occur in a shallow tunnel. The minimum peak

compressive stress seen is 8 MPa, which nevertheless is equivalent to 400 m of overburden – a situation never experienced by a shallow SCL tunnel in an urban environment.

Table 14

Interface minimum peak strengths for composite shell lining assuming spray-applied waterproofing membrane (*TamSeal 800*)

Interface Type	Compression MPa	Tension MPa	Shear MPa
Thin membrane, smoothed or regulated layer	30	0.7	2.1
Thin membrane, as-sprayed layer	11	0.7	2.0
Thick membrane, smoothed or regulated layer	10	0.7	2.0
Thick membrane, as-sprayed layer	8	0.7	1.7

Minimum peak tensile stress proposed is 0.7 MPa, 40% higher than the maximum water pressure on an SCL tunnel 50 m below ground level. The post-peak tensile capacity of 0.4 MPa at a membrane interface extension of 1.5 mm give confidence in the degree of ductility in the interface in tension. The minimum shear strength in Table 14 is similar to the stress (2 MPa) suggested by Pickett and Thomas (2011) to be potentially mobilised in a fully composite SCL tunnel under no-slip conditions. As discussed above, the interface shear stiffness has been observed to lie within the range where a degree of slip is expected (ibid.), such that the actual interface stress will be significantly less than 2 MPa. Furthermore, peak shear strength usually occurs at interface shear displacements of the order of 10-15 mm, which is a highly unlikely scenario for a shallow SCL tunnel. Taken together, these factors suggest the interface has sufficient shear strength to perform its function in providing partial composite action.

8 Conclusions

This research has investigated properties of the interface between sprayed concrete primary and secondary linings when a spray-applied waterproofing layer is used and tested under conditions of ambient humidity; properties needed for efficient design of composite SCL tunnels in soft ground. It

has been shown that neither of the key specified characteristics of the interface, namely membrane thickness and substrate roughness, has major impact on the measured interface properties of stiffness and strength, and their actual effect has been quantified in terms of proposed ranges of interface stiffness parameters K_n and K_s for design. It has also been demonstrated that sufficient robustness exists in the interface to resist any sudden loading changes. Consequently, the concrete-membrane-concrete interface of specified membrane thickness and substrate roughness may be simulated in numerical models by using interface elements, assigned with the interface parameters presented in this paper. This will significantly simplify numerical modelling of a composite SCL tunnel.

Although these parameters were developed from relatively few tests on samples with only one membrane type, the relative insensitivity of K_n and K_s to the interface characteristics and the wide ranges proposed should adequately cover most situations in practical SCL tunnel construction. For major tunnelling projects, these parameters could be used directly in an initial numerical investigation at feasibility study stage. Designers have the option to specify similar tests to the ones described in this paper, either prior to and during construction, to verify parameter values appropriate to their chosen membrane type and level of workmanship.

Further research is under way using the concrete-membrane-concrete interface parameter values presented in this paper to (1) develop a numerical modelling approach for a composite SCL lining, initially validated for a composite beam against laboratory test results, (2) apply the validated modelling approach to a whole SCL tunnel to understand its performance under various combinations of interface characteristics and loading, and (3) explore the degree of load sharing between the linings and the potential for lining thickness reduction in a composite SCL tunnel. In addition, to verify the appropriateness of the ‘dry’ humidity assumption for the membrane, in situ measurements of the membrane moisture content in a composite SCL tunnel in soft ground could be made. If the ‘dry’ condition was thought not to be representative of the field condition, element tests at the appropriate membrane moisture content should be carried out.

Acknowledgements

The authors gratefully acknowledge the financial support from Mott MacDonald and TAM-Normet for carrying out the investigation reported in this paper. The work was carried out at the University of Southampton with facilities provided by the Faculty of Engineering and the Environment.

Appendix

Table A1 Uniaxial compression test results

Sample designation	Membrane thickness (mm)	Peak Stress (MPa)	First loading stiffness (GPa/m)	Cyclic loading stiffness (GPa/m)
1-2	2.0	38	11.5	63.8
1-3	2.5	38	11.6	62.5
1-4	3.0	37	13.6	78.4
2-1	3.0	32	27.8	57.9
2-2	2.5	39	15.6	66.6
2-3	2.5	38	13.8	71.6
3-2	4.0	20	8.7	77.2
3-3	3.5	14	5.5	29.4
3-4	4.0	24	8.1	70.1
4-2	9.5	17	2.6	33.3
4-3	9.0	24	3.3	31.4
5-1	12.0	20	2.2	21.2
5-2	11.5	13	2.3	30.8
5-3	9.0	15	2.9	33.5
6-1	6.0	24	7.0	81.1
6-2	8.5	12	2.8	39.5
6-3	6.5	17	4.3	63.7

Table A2 Direct tension test results

Sample designation	Membrane thickness (mm)	Peak stress (MPa)	First loading stiffness (GPa/m)	Cyclic loading stiffness (GPa/m)
1-5	2.0	0.93	10.6	12.1
1-6	2.0	0.80	14.6	46.8
1-7	2.5	0.75	20.4	37.9
2-5	1.0	0.98	59.3	46.2
2-6	1.0	1.13	111.6	100.1
2-7	2.5	1.07	219.1	57.8
3-5	3.0	1.12	399.1	104.0
3-7	3.0	0.88	42.0	43.1
4-5	7.5	1.03	15.0	21.2
4-6	8.0	0.75	7.4	19.0

4-7	8.0	0.93	18.2	37.0
5-5	10.0	0.86	3.4	7.9
5-6	8.0	1.00	7.6	13.1
5-7	9.0	0.80	7.8	13.3
6-6	4.5	0.94	34.7	53.6
6-7	6.0	1.04	34.3	52.6

Table A3 Direct shear test results (under 500 kPa normal pressure)

Sample designation	Membrane thickness (mm)	Peak shear stress (MPa)	Shear displacement at peak stress (mm)	First loading stiffness (GPa/m)	Cyclic loading stiffness (GPa/m)
1-21	3.0	2.64	9.8	0.58	4.07
1-22	4.0	2.29	8.8	0.50	2.05
1-23	3.0	2.44	9.5	0.82	4.95
2-21	4.0	2.35	10.0	0.74	N/A
2-22	4.0	3.12	8.6	0.69	3.70
2-23	4.0	2.80	10.3	0.51	5.51
3-21	3.0	3.41	9.6	1.01	7.70
3-22	4.0	2.28	14.2	0.93	2.96
3-23	3.0	3.04	10.6	1.05	5.48
4-21	6.0	2.12	12.5	0.73	1.97
4-22	5.0	2.24	14.1	0.48	2.78
4-23	5.0	2.07	10.2	0.98	1.85
5-21	6.0	2.20	12.7	0.61	1.28
5-22	8.0	2.36	13.2	0.38	1.82
5-23	8.0	2.20	13.0	0.52	1.74
6-21	8.0	2.18	15.0	0.59	1.41
6-22	8.0	1.94	9.4	0.62	1.56
6-23	9.0	2.64	14.4	0.58	2.96

References

Ashby, M.F., Jones, D.R.H., 2005. Engineering Materials 2: An Introduction to Microstructures, Processing and Design, third ed. Butterworth-Heinemann, UK.

BS-EN 12390-1, 2000. Testing Hardened Concrete – Part 1: Shape, dimensions and other requirements for specimens and moulds. British Standards Institute, London.

BS-EN 14487-1, 2995.Sprayed Concrete – Part 1: Definitions, specifications and conformity. British Standards Institute, London.

Crossrail, 2009. Crossrail SCL Tunnels – MDC2/3 Sprayed Secondary Lining Study. Unpublished Report.

Dimmock, R.H., Haig, B., Su, J., 2011. Spray Applied Waterproofing Membranes – Key Success Factors and Development of Efficient Sprayed Concrete Tunnel Linings. In: Beck T, Woldmo O & Engen S, (Eds.), Sixth International Symposium on Sprayed Concrete, Tromso, Norway, pp. 110-124.

Duarte, P., Thomas, A.H., Cooke, M., 2012. Sustainability and the Tunnelling Industry. In: Kolic D, (Eds.), Under City Colloquium on Using Underground Space in Urban Areas in South-East Europe, Croatia, 2012. pp. 273-288.

Grose, W.J., Eddie, C.M., 1996. Geotechnical aspects of the construction of the Heathrow transfer baggage system tunnel. In: Mair, R., Taylor, N., (Eds.), Geotechnical Aspects of of Underground Construction in Soft Ground. Taylor & Francis, London, pp. 269-276.

Holter, K.G., Geving, S., 2015. Moisture transport through sprayed concrete tunnel linings. Rock Mech Rock Eng. DOI 10.1007/s00603-015-0730-1

Holter, K.G., 2016. Performance of EVA-Based Membranes for SCL in Hard Rock. Rock Mechanics and Rock Engineering, Volume 49, Issue 4, pp 1329-1358. DOI 10.1007/s00603-015-0844-5

Institution of Civil Engineers, 1996. Sprayed concrete linings (NATM) for tunnels in soft ground, ICE design and practice guide. Thomas Telford., London.

ITAtech, 2013. Design Guidance for Sprayed Applied Waterproofing Membranes. Int Tunn Assoc.

Kovári, K., 2003a. History of the sprayed concrete lining method – Part I: milestones up to the 1960s. Tunn. Undergr. Space Technol. 18, 57-69.

Kovári, K., 2003b. History of the sprayed concrete lining method – part II: milestones after the 1960s. Tunn. Undergr. Space Technol. 18, 71-83.

Nakashima, M., Hammer, A.L., Thewes, M., Elshafie, M. and Soga, K., 2015. Mechanical behaviour of a sprayed concrete lining isolated by a sprayed waterproofing membrane. Tunnelling and Underground Space Technology, 47, pp.143-152. http://dx.doi.org/10.1016/j.tust.2015.01.004.

Neville, A.M., 2011. Properties of Concrete, 5th ed. Prentice Hall, US.

Normet, 2011. Method Statement for the Installation of TamSeal 800 Sprayed Applied Waterproofing Membrane.

Peynolds, P., 2008. Hindhead Hit. Tunnels &Tunnelling International, October, pp.16-18.

Pickett, A.P., Thomas, A.H., 2011. The design of composite shell linings. In: Beck T, Woldmo O & Engen S, (Eds.), Sixth International Symposium on Sprayed Concrete, Tromso, Norway, pp.402-413

Su, J., Thomas, A,. 2014. Design of Sprayed Concrete Lining in Soft Ground – A Crossrail perspective. In: Black M, Dodge C & Laurence U, (Eds.), Crossrail Project: Infrastructure design and construction, volume 1. London, GB, ICE Publishing. pp.123-136

Thomas, A.H., 2009. Sprayed Concrete Lined Tunnels. Taylor & Francis, London.

Verani, C.A., Aldrian, W., 2010. Composite linings: ground support and waterproofing through the use of a fully bonded membrane. In: Bernard, E.S., (Eds.), Shotcrete: Element of a System. Taylor & Francis, London, pp. 269-282.

Watson, P.C., Warren, C.D., Eddie, C.M., Jager, J., 1999. CTRL North Downs Tunnel. In: Tunnel Construction and Piling ‘99. The Hemming Group, London, pp. 301-323.

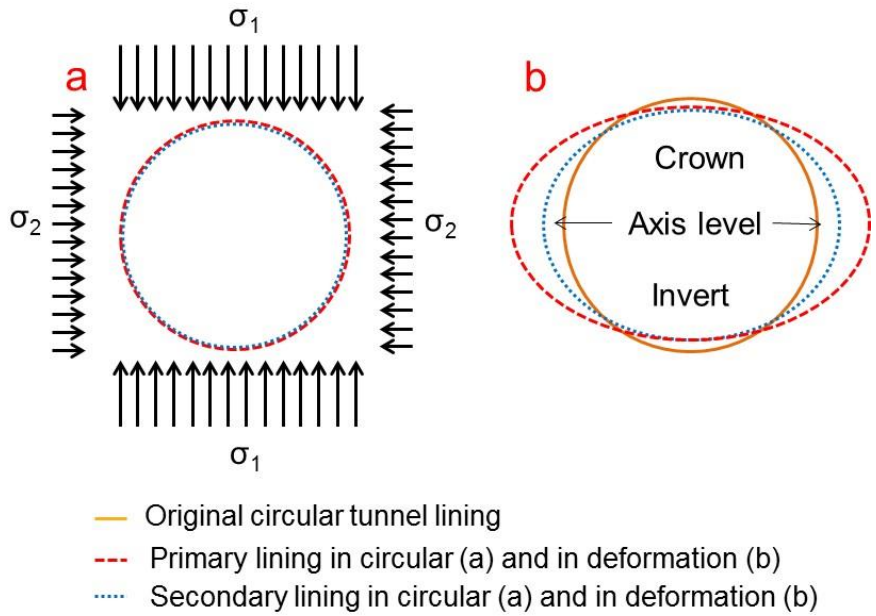

Figure 1 (a) idealised perfectly circular composite SCL tunnel with applied ground loading, and (b) typical resulting lining deformation.

Figure 2 Spray operations at contractor’s yard

Figure 3 Left to Right: as-sprayed, smoothed and regulated surface finishes, Top to Bottom: before and after application of TamSeal 800 spray applied waterproofing membrane

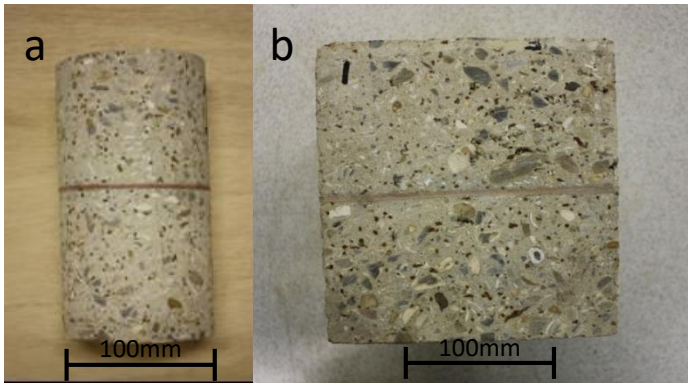

Figure 4 Typical (a) cylinder sample and (b) cube sample

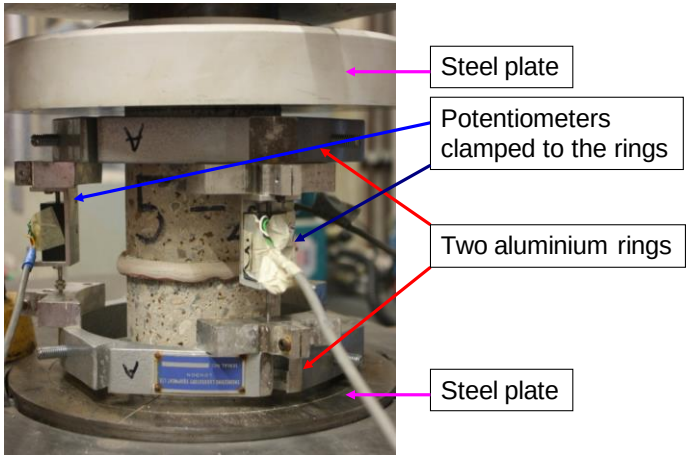

Figure 5 Typical compression test setup

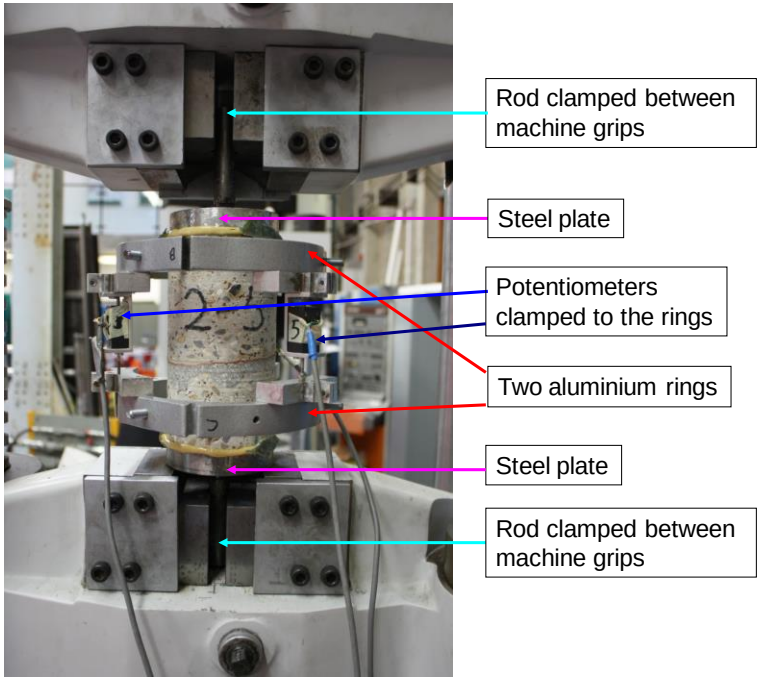

Figure 6 Typical direct tension test setup

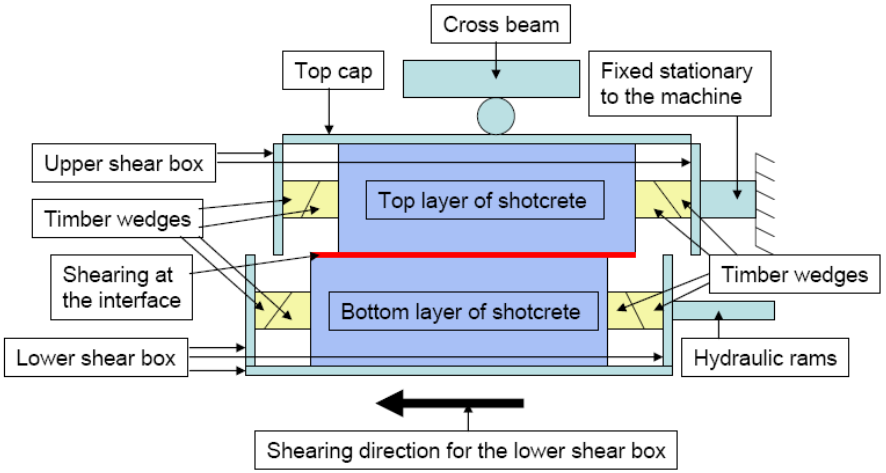

Figure 7 Schematic of direct shear test

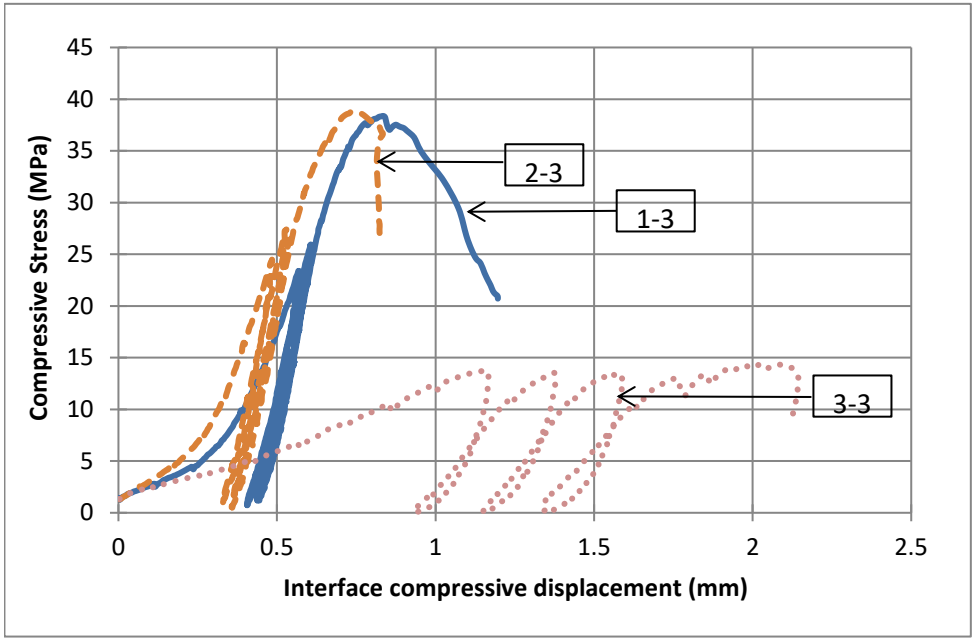

Figure 8 Thin membrane interface behaviour in uniaxial compression

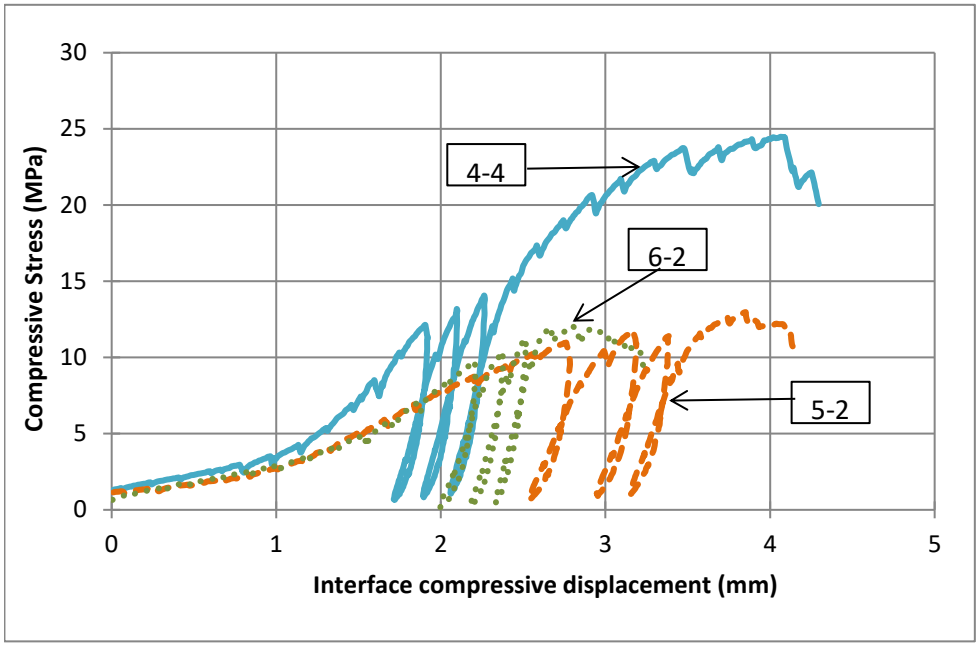

Figure 9 Thick membrane interface behaviour in uniaxial compression

Figure 10 Typical compressive failure modes for (a) thin membrane interface (b) thick membrane interface

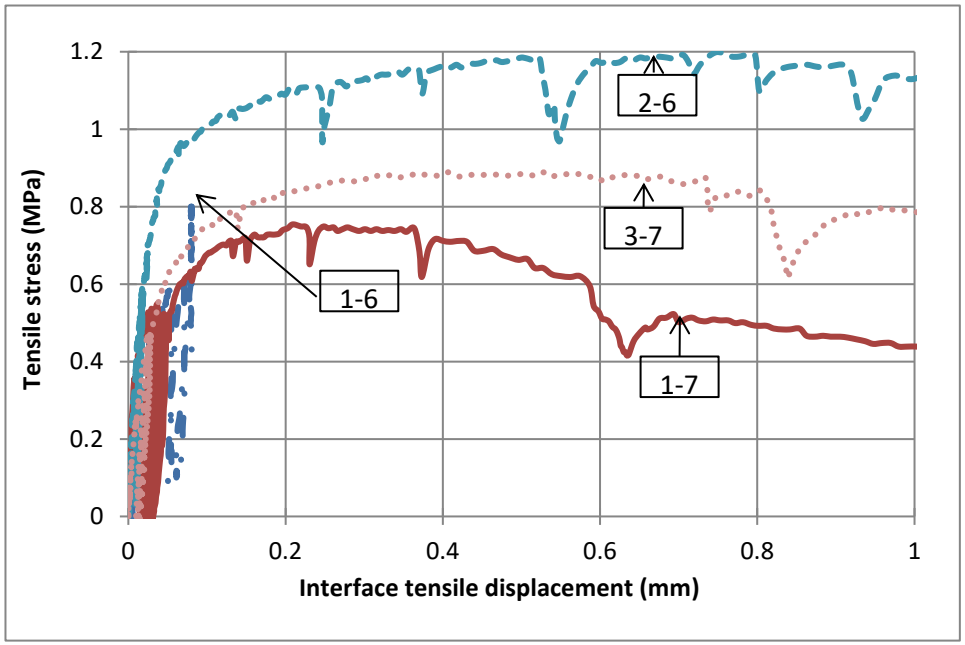

Figure 11 Thin membrane interface behaviour in direct tension

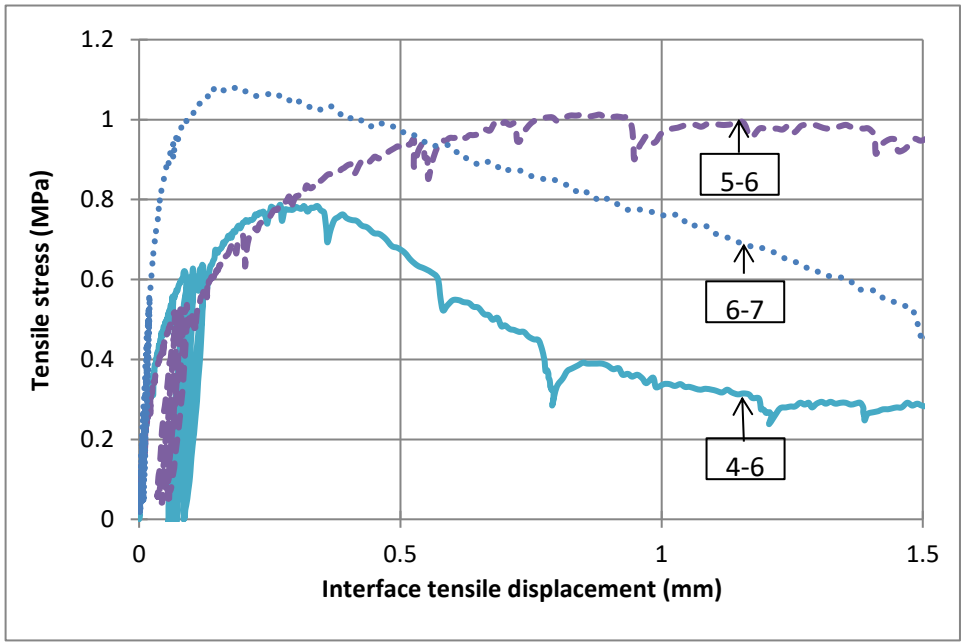

Figure 12 Thick membrane interface behaviour in direct tension

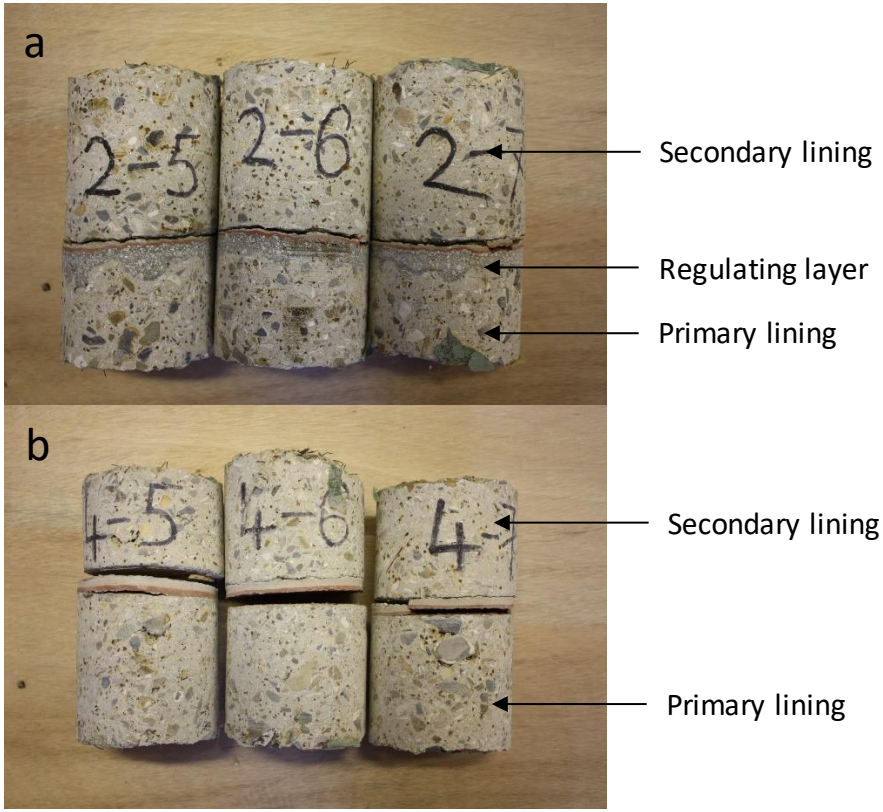

Figure 13 (a) membrane bonding to regulating layer and debonded from secondary lining (b) equal probability of debonding from primary or secondary linings if no regulating layer present

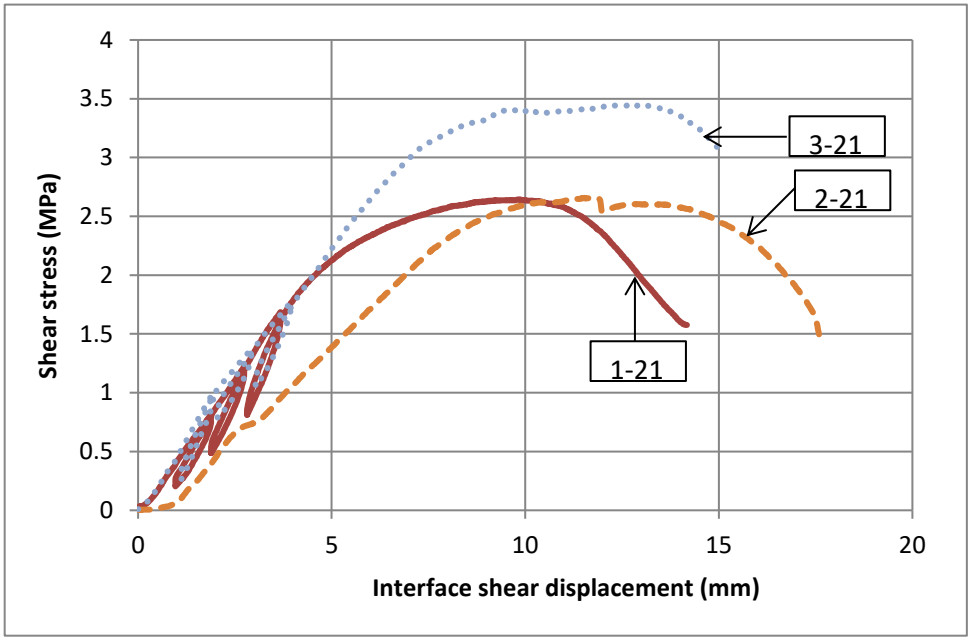

Figure 14 Thin membrane interface behaviour in direct shear under 500 kPa normal pressure

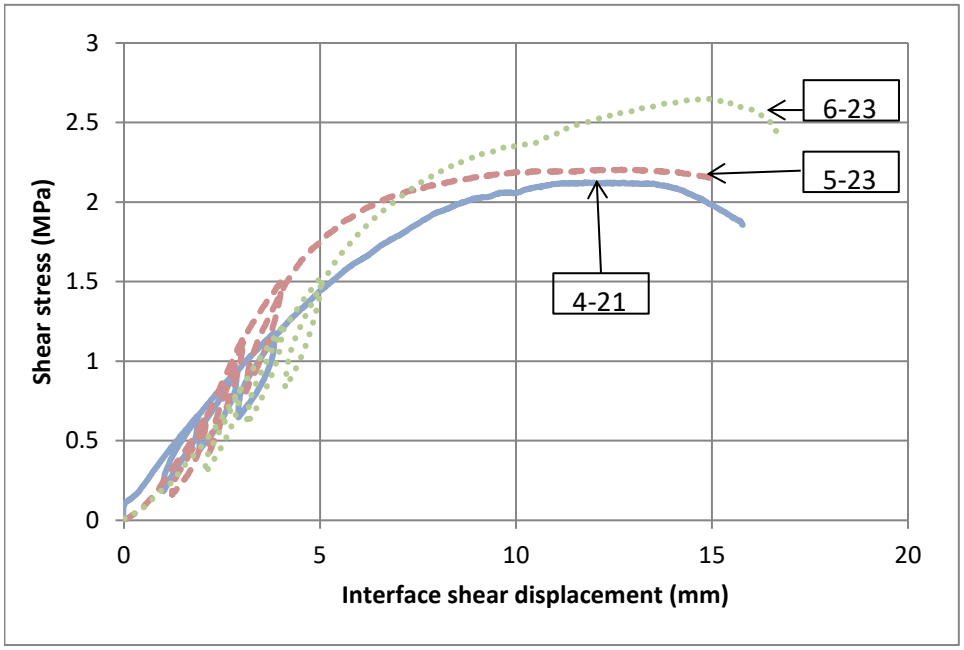

Figure 15 Thick membrane interface behaviour in direct shear under 500 kPa normal pressure

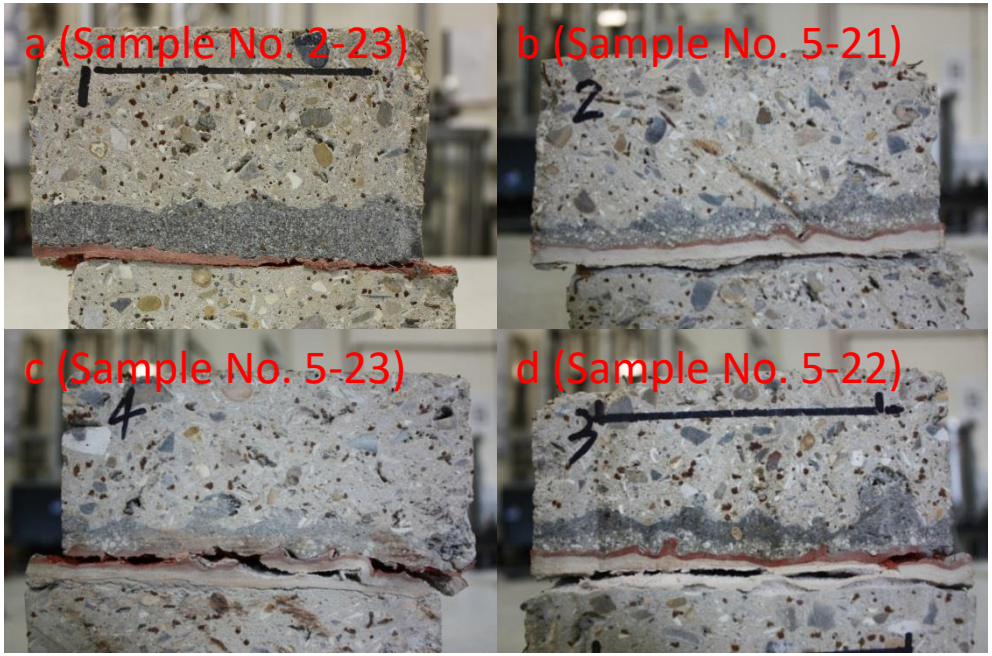

Figure 16 Typical failure modes under direct shear test

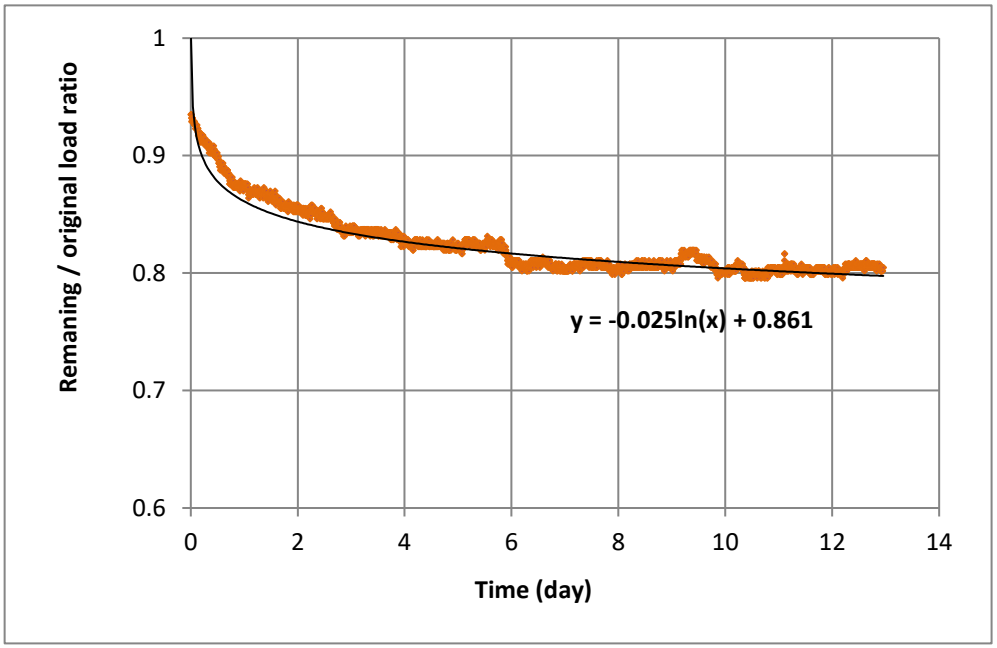

Figure 17 Typical load relaxation-time relationship for a Type 2 interface under long-term shear loading